CONTROL POWER MINIMIZATION OF BALLOON-TELESCOPE SYSTEMS

by

Melvin F. Diels

A Thesis Submitted to the Faculty of the

DEPARTMENT OF AEROSPACE AND MECHANICAL ENGINEERING

In Partial Fulfillment of the Requirements
For the Degree of

MASTER OF SCIENCE

In the Graduate College

THE UNIVERSITY OF ARIZONA

1 9 6 4

STATEMENT BY AUTHOR

This thesis has been submitted in partial fulfillment of requirements for an advanced degree at the University of Arizona and is deposited in the University Library to be made available to borrowers under rules of the Library.

Brief quotations from this thesis are allowable without special permission, provided that accurate acknowledgment of source is made. Requests for permission for extended quotation from or reproduction of this manuscript in whole or in part may be granted by the head of the major department or the Dean of the Graduate College when in their judgment the proposed use of the material is in the interests of scholarship. In all other instances, however, permission must be obtained from the author.

SIGNED: Melvin F. Diels

APPROVAL BY THESIS DIRECTOR

This thesis has been approved on the date shown below:

Roger A. Anderson — 2 January, 1964

ROGER A. ANDERSON — Date

Professor of Aerospace and Mechanical Engineering

ACKNOWLEDGMENTS

The author wishes to express his gratitude to the Institute of Atmospheric Physics and the Applied Research Laboratory of the University of Arizona for the opportunity of being able to both pursue graduate studies and also participate in the "Polariscope I" program, a part of which has made this thesis possible. He also wishes to express his appreciation to Dr. R. A. Anderson for his helpful suggestions in the preparation of this thesis.

TABLE OF CONTENTS

TABLE OF CONTENTS (Concluded)

ILLUSTRATIONS

ABSTRACT

Control power requirements for balloon-telescope systems are considered for various telescope mounting configurations. The equations of motion about the azimuth axis of a three-axis system are developed and performance is optimized to give a minimum required control power. Applications are made to the "Polariscope I" balloon-telescope system.

I. INTRODUCTION

Very high altitude balloon flights are achieved by maximum weight reduction of both the balloon and payload. One of the larger weight items in balloon-telescope systems is the power source, which is usually composed of batteries. Other sources, such as nuclear power, may be required for very large telescope systems. The power consumed by the electrical components and the duration of flight determine the quantity of batteries required. Considerable amounts of electrical power are consumed by the control motors which stabilize the telescope, and any reduction in this electrical power notably reduces the total weight of the system. Therefore, methods of achieving weight reduction by this technique have been investigated in this analysis.

Methods of telescope mounting, arrangement of the axes of rotation, and various means of stabilization are considered on the basis of minimum weight. The best of these methods is extensively analyzed to determine the optimum configuration which uses minimum control power. This configuration has been applied to the design of the "Polariscope I" balloon-telescope system.

II DISCUSSION OF BALLOON-TELESCOPE SYSTEMS

Placement of large astronomical telescopes above the earth's atmosphere, where viewing is unimpaired, is a logical extension in experimental astronomy. Several means are available for doing this at the present time. The use of large balloons to lift these astronomical instruments to very high altitudes is one available method. Another means is to rocket launch them either for short-duration flight or into a satellite orbit in space above the earth's atmosphere. Both methods require a stabilized platform to hold the telescope in fixed orientation while viewing a given object in space. A remotely controlled, gyro-stabilized system is required. These systems are expensive and very complicated. A balloon launched telescope system is considerably less expensive than the orbiting satellite, but the viewing time per flight is much less. However, many experiments require a relatively short viewing time, and therefore balloon-telescope systems are quite advantageous.

Many configurations of the telescope stabilization platform are possible. A minimum of two axes of rotation is required in order that the telescope can be fixed on any point in the sky and be controlled to that point. These two axes of rotation are arranged so that they are perpendicular to each other, and can be oriented in any convenient manner in the gondola. A much used orientation, such as "Stratoscope I", shown in Figure 2.1, has an azimuth axis and an elevation axis. The elevation axis is fixed horizontally in the gondola, and the telescope is able to rotate about this axis from a horizontal to a vertical viewing position. The telescope and the gondola rotate as a unit about the vertical azimuth axis. A disadvantage of this arrangement is the high moment of inertia about the azimuth axis, as the whole gondola must be rotated along with the telescope for motion about this axis. This high inertia requires more control power, and thus more battery weight, than a system in which only the telescope has to move. Such a system requires a third axis of rotation. The telescope is mounted inside a gimbal ring which allows motion about both an elevation and a cross-elevation axis. This configuration is shown in Figure 2.1. The moments of inertia about both axes are thus small. The elevation axis is again fixed

horizontally in the gondola, and the gimbal ring is able to rotate about this axis. The cross-elevation axis is fixed in the gimbal ring at right angles to the elevation axis, and the telescope is able to rotate about this axis through a small angle. The telescope and the gimbal ring rotate as a unit about the elevation axis. The third axis would be again the vertical azimuth axis in the gondola. If the control on the azimuth axis were an intermittent one, with the azimuth control motor being required to operate only a small percentage of the time, the total control power required would be less than that required for the two-axis system. This is the type of three-axis system which will be optimized in this thesis. A more complete discussion of various balloon-telescope systems is presented in Reference 1.

Several external torques about the azimuth axis of three-axis balloon-telescope systems can be exerted on the gondola or the telescope. Rotation of the balloon will produce a torque at the connecting link between the shroud lines and the gondola. An aerodynamic torque will be produced on the telescope by a side wind blowing on the system or by the pendulum motion of the gondola swinging below the balloon as it moves through the air. A gravitational

torque will be produced during pendulum motion if the center of gravity of the system is not located on the azimuth axis.

The torque produced by rotation of the balloon on the connecting link should be as low as possible, so that minimum external torque will be transmitted to the system. If there were a frictionless link between the shroud lines and gondola, there would be no effect produced by the balloon rotation on the gondola. The torques produced by the aerodynamic moment and the gravitational unbalance can be counteracted by acceleration of an inertia wheel or by reaction jets. The system to be considered here employs an inertia wheel which is shown with respect to the rest of the system in Figure 2.2. If acceleration of the inertia wheel continues for prolonged periods of time, the inertia wheel will eventually reach its maximum rotational speed and hence become ineffective. A means of ridding the inertia wheel of its angular momentum must be supplied if the azimuth control is to remain effective. The best inertial sink for the wheel momentum is the balloon itself, which has a very large moment of inertia as compared to the inertia wheel.

The inertia wheel momentum must be transferred by friction, through the rotating connecting link and into the shroud lines. The amount of this frictional torque should be just sufficient to transfer the excess momentum supplied to the inertia wheel by the aerodynamic and gravitational unbalanced torques. The effect of balloon rotation on the system is thus minimized. The shroud lines must have an adequate spring constant to resist the connecting link friction torque so that the inertia wheel's excess momentum can be transferred to the balloon. Also the shroud lines must be stiff enough so that they do not wind up into a rope-like configuration which can resist only a very small amount of torque. Stiffness of the shroud lines is achieved by employing a large spacing between the individual shroud lines at the connecting link.

A nonrotating connecting link could be used on balloon-telescope systems, but this type of link would be very wasteful of azimuth control power, and would also cause the azimuth control to be less stable in operation. This type of connecting link has therefore not been considered in this analysis.

III DEFINITION OF SYSTEM

3.1 Model of Azimuth System

A schematic model showing the components which significantly affect the azimuth angular motion of three-axis balloon-telescope systems is given in Figure 3.1. The three inertial masses of the balloon, inertia wheel and gondola are shown. The angular positions of the various components are shown in their respectively defined positive directions. The various torques which exist on the system are also shown in their positive directions. And the torsional spring constant of the shroud line suspension system is shown.

The azimuth drive system, shown in Figure 3.2, is composed of three components: the azimuth shaft, the control motor, and the gear box. The inertia wheel is rigidly fastened to the azimuth shaft. The shaft is mounted in bearings to the gondola. The gear box and the control motor are mounted to the gondola, and drive the shaft. Rotation of the control motor produces relative motion between the gondola and the inertia wheel. Whenever there is relative motion between the two, the control

motor shaft is rotating. During this motion the control motor may or may not be supplying torque to the system. If no torque is being supplied, the friction in the bearings of the azimuth shaft, the gear box, and the control motor tends to stop the relative motion between the gondola and inertia wheel. This frictional torque is always opposing the relative rotational motion while the control motor may supply torque in either the same or the opposite direction. The resultant torque on the system when the motor is operating may therefore be greater than, or less than the ideal torque produced by the motor and gear box. This resultant torque depends upon the type of motion which prevails. Thus, the frictional torque and the ideal control motor torque must be treated separately in this system.

The general conditions which have been assumed for the azimuth system are presented below. The moment of inertia of the balloon is assumed to be very large in comparison to the moments of the gondola or the inertia wheel. The weight of the balloon is approximately equal to that of the sum of the inertia wheel and gondola, and most of this weight is located at a very large radius, thus making the moment of inertia of the balloon very

large compared to that of either the gondola or of the inertia wheel. The moments of inertia of the gondola and inertia wheel are assumed to be in the same order of magnitude.

The azimuth motor-gear box output torque is assumed to be greater than the frictional torque of the azimuth shaft and gear box; this is required of the azimuth motor for it to be effective in rotating the azimuth system. The frictional torque of the azimuth shaft and gear box is assumed to be greater than that of the connecting link. And the frictional torque of the connecting link is assumed to be greater than the torque produced by the aerodynamic and gravitational unbalances. This last assumption is required so that stability of the azimuth system prevails. All of the angular momentum produced by the unbalanced torques must be transferred through the shroud lines to the balloon with its very large moment of inertia to give the system stability. The shroud lines must have a large spring constant so that they can resist the connecting link frictional torque without winding up into a rope which would be unable to resist any appreciable amount of torque. These assumptions result in nearly the same angular positions of the connecting link and the balloon.

Three types of angular motion of the azimuth system are possible with the above assumptions:

a. The gondola, the inertia wheel and the balloon all have different angular velocities.

b. The gondola and the inertia wheel have the same angular velocity while the balloon has a different velocity.

c. The gondola, the inertia wheel and the balloon all have the same angular velocity.

Motion with the same balloon and inertia wheel velocities and a different gondola velocity is not possible with the above assumption that the connecting link frictional torque is less than that of the azimuth shaft and gear box. Once the gondola and the inertia wheel reach the same velocity they rotate together as a unit if the azimuth motor is off. The frictional torque produced by the connecting link is not great enough to cause relative motion between the inertia wheel and the gondola. Thus relative motion between the connecting link and the inertia wheel must continue until some time after the relative motion between the inertia wheel and the gondola ceases. Motion with the same gondola and balloon velocities and a different inertia wheel velocity has no significance for this system.

3.2 Sign Convention

The following sign convention is employed in this analysis:

a. The angular positions of the gondola, the inertia wheel, the balloon and the connecting link are all positive in the same direction.

b. The connecting link frictional torque is positive if it produces positive acceleration of the inertia wheel.

c. The aerodynamic and gravitational unbalance torque, the frictional torque of the azimuth shaft and gear box, and the azimuth motor-gear box output torque are all positive if they produce positive acceleration of the gondola.

3.3 Azimuth Shaft and Gear Box Friction

The assumed characteristics of the frictional torque produced in the azimuth shaft and gear box are presented in Figure 3.3. The absolute value of this frictional torque is assumed to be constant. The torque is positive when the difference of the velocities of the inertia wheel and of the gondola is positive, and negative when the difference is negative. The use of antifriction ball bearings with only a thin film of silicon oil on them is assumed. Friction is thus reduced to a minimum at the sub-zero temperatures encountered by balloon-telescope systems which operate at altitudes above twenty miles. The assumption of Coulomb friction is thus a good one for this type of bearing with minimum lubrication. No lubrication would be theoretically required of these bearings, as their life and rotational speed is very low, but a thin film of oil is required to stop corrosion.

3.4 Connecting Link Friction

The assumed characteristics of the connecting link frictional torque are shown in Figure 3.4. The absolute value of this torque is assumed constant for Coulomb friction. The torque is positive when the difference of the balloon and the inertia wheel velocities is positive.

3.5 Characteristics of the Azimuth Motor and Gear Box

The assumed azimuth motor-gear box output torque characteristics are shown in Figure 3.5. The absolute value of the torque output, when the azimuth motor is on, is assumed constant. The torque is zero when the motor is off. The azimuth motor is assumed to go on and off at some given absolute values of the gondola angular position. The output torque, when the motor is on, is negative for positive gondola positions and vice versa.

3.6 Aerodynamic and Gravitational Unbalance

When the telescope is in a nearly horizontal viewing position, there will be an aerodynamic unbalanced torque produced about the azimuth axis of the gondola if a relative wind is blowing sideways on the telescope light shield. Pendulum motion of the gondola below the balloon can also produce a side wind and thus an aerodynamic torque on the telescope.

If the center of gravity of the gondola and inertia wheel does not lie on the azimuth axis of the system, a torque due to the gravitational unbalance will be produced about the azimuth axis when the gondola is moving in pendulum motion below the balloon.

Another torque which is present on the gondola is caused by reaction of the gimbal control motors. This torque is produced about the cross-elevation axis of the telescope, as this axis, unlike the elevation axis, is not perpendicular to the azimuth axis. The cross-elevation axis is perpendicular to the elevation axis only. The period of the cross-elevation motion is assumed to be short compared to the period of the azimuth motion, as the telescope controls hold the telescope in a nearly fixed position

in space at all times. Thus the telescope reaction torque is assumed to have no net effect on the azimuth axis motion.

3.7 Balloon Motion

The torsional period of motion for balloons of ten million cubic feet volume which are used for lifting large balloon-telescope systems is about 15 minutes, according to Reference 2. This balloon period is much longer than the period of azimuth motion, thus the assumption has been made in this analysis that the balloon angular velocity can be treated as a constant. The maximum angular velocity of the balloon from experimental data given in Reference 2 is about one degree per second, (.02 radians per second).

IV DEVELOPMENT OF EQUATIONS OF MOTION

4.1 Motion About the Azimuth Axis

The law governing angular motion about an axis, which is similar to Newton's second law for linear motion of a constant mass, can be stated as follows: the summation of all external torques on a body must be equal to the product of the moment of inertia of the body and the angular acceleration of the body.

$$\Sigma T = I\ddot{\theta}$$

The definition of symbols used is presented in the List of Nomenclature.

Employing the sign conventions given in Chapter III along with the conditions and assumptions presented there, two angular equations of motion about the azimuth axis of balloon-telescope systems can be written. The gondola motion equation is as follows:

$$(T_a + T_b + T_M) = I_G \ddot{\theta}_G$$

and that of the inertia wheel is:

$$[T_c - (T_b + T_M)] = I_W \ddot{\theta}_W$$

Combining these two equations gives the general equation of motion about the azimuth axis of balloon-telescope systems.

$$(T_b + T_M) = (I_G \ddot{\theta}_G - T_a) = -(I_W \ddot{\theta}_W - T_c) \qquad 4.1$$

4.2 Motion During Interval With $(\dot{\theta}_G \neq \dot{\theta}_W \neq \dot{\theta}_B)$

The first type of angular motion about the azimuth axis of balloon-telescope systems is one in which the gondola, inertia wheel and balloon all have different angular velocities. The equations of motion for this type of operation are derived by solving for the two accelerations in Equation 4.1. These are:

$$\ddot{\theta}_G = \left[\frac{(T_a + T_b + T_M)}{I_G}\right] = \alpha_G \qquad 4.2$$

and

$$\ddot{\theta}_W = \left[\frac{T_c - (T_b + T_M)}{I_W}\right] = \alpha_W \qquad 4.3$$

The angular velocities of the gondola and the inertia wheel can be determined by integration of these equations with respect to time. It is assumed that all of the torques are constant during the time interval being considered, and time is measured from the beginning of the interval. The gondola angular velocity is derived from Equation 4.2.

$$\dot{\theta}_G = (\dot{\theta}_G)_0 + (\alpha_G)t \qquad 4.4$$

From Equation 4.3, the angular velocity of the inertia wheel is determined.

$$\dot{\theta}_W = (\dot{\theta}_W)_0 + (\alpha_W)t \qquad 4.5$$

Angular positions of the gondola and of the inertia wheel are determined by integration of Equations 4.4 and 4.5. They are:

$$\theta_G = (\theta_G)_0 + (\dot{\theta}_G)_0 t + (\alpha_G)\frac{t^2}{2} \qquad 4.6$$

and

$$\theta_W = (\theta_W)_0 + (\dot{\theta}_W)_0 t + (\alpha_W)\frac{t^2}{2} \qquad 4.7$$

4.3 Motion During Interval With $(\dot{\theta}_G = \dot{\theta}_W \neq \dot{\theta}_B)$

A second type of angular motion about the azimuth axis of balloon-telescope systems is one in which the gondola and inertia wheel have the same angular velocity, while the balloon has a different velocity. This type of operation can occur only when the azimuth motor is not operating. Solving Equation 4.1 with $(\ddot{\theta}_G = \ddot{\theta}_W)$ and $(T_M = 0)$ gives

$$\ddot{\theta}_G = \ddot{\theta}_W = \left(\frac{T_a + T_c}{I_G + I_W}\right) = \alpha_{GW} \qquad 4.8$$

Integration with respect to time, assuming constant torques and zero initial time, gives the angular velocity of the gondola and the inertia wheel.

$$\dot{\theta}_G = \dot{\theta}_W = (\dot{\theta}_G)_0 + (\alpha_{GW})t \qquad 4.9$$

Integrating again gives the angular positions

$$\theta_G = (\theta_G)_0 + (\dot{\theta}_G)_0 t + (\alpha_{GW})\frac{t^2}{2} \qquad 4.10$$

and

$$\theta_W = \theta_G - (\theta_G)_0 + (\theta_W)_0 \qquad 4.11$$

These two equations are not the same because the initial positions of the gondola and of the inertia wheel are different.

4.4 Motion During Interval With $(\dot{\theta}_G = \dot{\theta}_W = \dot{\theta}_B = \text{Constant})$

A third type of angular motion about the azimuth axis is one in which the gondola, inertia wheel and balloon all have the same angular velocity. The azimuth motor is inoperative for this type of motion, and in Section 3.7, a constant angular velocity of the balloon was assumed. Thus, the gondola and inertia wheel accelerations are equal to zero, i.e.,

$$\ddot{\theta}_G = \ddot{\theta}_W = 0$$

Integrating twice with respect to time for constant torques and zero initial time gives:

$$\theta_G = (\theta_G)_0 + (\dot{\theta}_B)t \qquad 4.12$$

and

$$\theta_W = (\theta_W)_0 + (\dot{\theta}_B)t \qquad 4.13$$

These two equations are not identical, as the two initial positions are different.

4.5 End Condition for Interval With $(\dot{\theta}_G \neq \dot{\theta}_W \neq \dot{\theta}_B)$

Four different interval end conditions can occur because of a torque change:

a. The gondola and inertia wheel can reach the same angular velocity

b. The inertia wheel and balloon can reach the same angular velocity

c. The azimuth motor can go off

d. The azimuth motor can go on

The time at which the gondola and the inertia wheel velocities are identical at the end of the interval is derived from Equations 4.4 and 4.5

$$t_{i(\dot{\theta}_G = \dot{\theta}_W)} = \left[\frac{(\dot{\theta}_W)_0 - (\dot{\theta}_G)_0}{(\alpha_G - \alpha_W)}\right] \qquad 4.14$$

The time at which the inertia wheel and balloon have the same velocity at the end of the interval is found from Equation 4.5.

$$t_{i(\dot{\theta}_W = \dot{\theta}_B)} = \left[\frac{(\dot{\theta}_B) - (\dot{\theta}_W)_0}{\alpha_W}\right] \qquad 4.15$$

The time at which the azimuth motor goes off at the end of the interval is derived from Equation 4.6. This

time occurs when $[\theta_G = (\theta_G)_{OFF}]$ as explained in Section 3.5.

$$t_i[\theta_G=(\theta_G)_{OFF}] = \left\{-\left[\frac{(\dot{\theta}_G)_0}{\alpha_G}\right] \pm \sqrt{\left[\frac{(\dot{\theta}_G)_0}{\alpha_G}\right]^2 - \left(\frac{2}{\alpha_G}\right)\left[(\theta_G)_0 - (\theta_G)_{OFF}\right]}\right\} \quad 4.16$$

The time at which the azimuth motor goes on at the end of the interval is also derived from Equation 4.6. This time occurs when $[\theta_G = (\theta_G)_{ON}]$

$$t_i[\theta_G=(\theta_G)_{ON}] = \left\{-\left[\frac{(\dot{\theta}_G)_0}{\alpha_G}\right] \pm \sqrt{\left[\frac{(\dot{\theta}_G)_0}{\alpha_G}\right]^2 - \left(\frac{2}{\alpha_G}\right)\left[(\theta_G)_0 - (\theta_G)_{ON}\right]}\right\} \quad 4.17$$

Six different values of time can be determined from the above four equations, 4.14 to 4.17. Of these possible times, only the lowest positive real one is of interest and significance, and it is the correct time for the end of the interval.

4.6 End Condition for Interval with $(\dot{\theta}_G = \dot{\theta}_W \neq \dot{\theta}_B)$

Only one end condition can occur for this type of motion: the azimuth motor goes on. The time at which this occurs is derived from Equation 4.10.

$$t_i[\theta_G=(\theta_G)_{ON}] = \left\{-\left[\frac{(\dot{\theta}_G)_0}{\alpha_{GW}}\right] \pm \sqrt{\left[\frac{(\dot{\theta}_G)_0}{\alpha_{GW}}\right]^2 - \left(\frac{2}{\alpha_{GW}}\right)\left[(\theta_G)_0 - (\theta_G)_{ON}\right]}\right\} \quad 4.18$$

The lowest positive real time of the two possible values is the desired time.

4.7 End Condition for Interval with $(\dot{\theta}_G = \dot{\theta}_W = \dot{\theta}_B = \text{Constant})$

Again, only one end condition occurs for this type of motion, namely, the azimuth motor goes on. The time at which this occurs is derived from Equation 4.12.

$$t_i[\theta_G = (\theta_G)_{ON}] = \left[\frac{(\theta_G)_{ON} - (\theta_G)_O}{\dot{\theta}_B}\right] \qquad 4.19$$

4.8 Typical Azimuth Control Cycle

Typical accelerations of the gondola and of the inertia wheel of balloon-telescope systems are shown in Figure 4.1 for a complete control cycle. The beginning and the end of the cycle occur at two successive points when the azimuth control motor goes on. The three types of motion during intervals and five of the possible six interval end conditions are shown.

The time during the cycle is given by the following expression:

$$\Sigma t = (t_O)_n + t \qquad 4.20$$

and the total cycle time for the azimuth motion of balloon-telescope systems is:

$$t_\tau = \sum_1^{n_\tau} t_i \qquad 4.21$$

4.9 Motion of Balloon

The angular position of the balloon is given by the following formula for a zero initial angle and a constant angular velocity:

$$\theta_B = (\dot{\theta}_B)\Sigma t \qquad 4.22$$

where Σt is given by Equation 4.20.

4.10 Calculation Procedure

The procedure for calculating the azimuth motion of balloon-telescope systems is presented in Table 4.1. The calculation proceeds one line at a time, where each line represents one time interval of the motion. The end conditions of each interval must first be determined before proceeding to the next interval, as the initial conditions of any interval are the end conditions of the previous interval. Steady-state motion must be determined by making a series of calculations. Many complete cycle calculations may have to be performed before the cycle end conditions are found to be the same as the initial conditions.

V "POLARISCOPE I" APPLICATION

5.1 Discussion

"Polariscope I" is a remotely controlled, gyro-stabilized telescope system which is to be launched by balloon to an operating altitude of 116,000 feet. The launch will be made from the bottom of Glen Canyon, just downstream from the nearly completed Glen Canyon Dam on the Colorado River in northern Arizona. Several flights are planned for the winter of 1963-64. The primary telescope mirror has a diameter of 71 centimeters, or about 28 inches. The project was awarded by the National Science Foundation to the Institute of Atmospheric Physics of the University of Arizona.

The over-all purpose of these flight experiments is to extend polarimetry and photometry in the study of diffuse radiation within atmospheres of the planets, and of the stars and space. At present a fair amount is known in the visible spectrum. These experiments will be made in the ultraviolet region between 2000 and 3000 Å.

The photometry part of the experiments basically measures the brightness of the collected light at various wave lengths. Organic-solution and interference filters are used to separate selected wave-length bands. The polarimetry part of the experiment employs a Wollaston prism. The shape of the polarization curve received is used to determine the size and the refractive index of the particles present in the atmosphere. In general, the results of these experiments will not show the composition of either the atmosphere or of the particles in the atmosphere. Presence of particles, their size and the depth of the atmosphere only will be determined. The diffuse radiation from dust and gases within the atmospheres of planets, stars, and the interstellar and planetary space will be studied. Reference 3 gives a more complete discussion of these experiments.

An operating altitude of 116,000 feet was chosen so that the experiments would not be affected by the ozone layer in the earth's atmosphere. This ozone layer is mostly below 116,000 feet only during the winter months; the flights will therefore be made only during that time of year. These high-altitude requirements necessitate the use of the largest available balloons and light payloads. The balloon to be used for "Polariscope I" flights will be three hundred feet in diameter, and will contain ten million cubic feet of helium at operating altitude. The suspension system will be the landing parachute and its shroud lines extended to 175 feet.

The inertia wheel is composed of 600 pounds of nickel-cadmium batteries located at the outer periphery of the wheel so as to produce the largest moment of inertia. The batteries perform three functions for the system: electrical power, inertial mass, and landing ballast. For this last purpose, individual battery units with parachutes can be jettisoned. Relative motion between the inertia wheel and gondola is produced by the azimuth motor and gear train; the gondola is thus caused to rotate about the azimuth axis.

The telescope has a three-axis of motion system. Two axes are located on the telescope gimbal, allowing motion of the telescope in elevation and cross-elevation. The third is the gondola azimuth axis. The telescope is gyro-stabilized about the two gimbal axes and has a Cassegrain mirror system. The f/2 primary mirror is 71 centimeters in diameter, and the Cassegrain focus is f/13. The secondary mirror at the forward end of the telescope has a diameter of 13 centimeters. The main advantage of this type of mirror system is its short, compact shape. The collected data are telemetered back to the ground station.

The gondola is a space-frame configuration designed by the author, and is constructed of thin-walled aluminum tubing. This type of construction makes for a very strong and yet light structure, a requirement of high-altitude balloon flights. The gondola frame weighs 120 pounds. The design allows 180 degrees of elevation motion and 20 degrees of cross-elevation motion of the telescope. The landing struts are of new design by the author. They employ telescoping tubes containing styrofoam pads which progressively crush to absorb the landing shock.

5.2 Assumptions and Variables

The assumed constants of the azimuth motion of the "Polariscope I" balloon-telescope system are presented in this section. Design optimization of the system produced a moment of inertia for the inertia wheel of 180 ft. lb. sec.^{2} and a gondola moment of inertia of 150 ft. lb. sec.^{2}.

The frictional torque produced in the connecting link should be as low as possible so as to minimize the effect of the balloon rotation on the gondola motion. This torque must also be greater than the maximum torque produced by the sum of the aerodynamic and gravitational unbalance torques. A maximum of .2 ft. lb. was determined for the aerodynamic and gravitational unbalance torque. Thus a connecting link frictional torque of .25 ft. lb. was chosen.

The gondola angle at which the azimuth motor goes on must be considerably less than the ten degrees maximum angle the telescope is able to travel in cross-elevation motion from the neutral position. A value of .1 radian has been chosen for the gondola angle at which the azimuth motor goes on. An ideal azimuth motor-on torque of 5.25 ft. lb. is produced at the output of the azimuth gear box and an azimuth shaft and gear box frictional torque of .5 ft. lb. occurs.

A summary of the various assumed constants used in this analysis follows:

I_G = 150 ft. lb. sec.^{2}

I_W = 180 ft. lb. sec.^{2}

$|T_\alpha|_{MAX}$ = .20 ft. lb.

$|T_b|$ = .50 ft. lb.

$|T_c|$ = .25 ft. lb.

$(T_M)_{OFF}$ = 0 ft. lb.

$|(T_M)_{ON}|$ = 5.25 ft. lb.

$|\dot{\theta}_B|_{MAX}$ = .02 rad./sec.

$|(\dot{\theta}_G)_O|_{MAX}$ = .07 rad./sec.

$|\theta_G|_{MAX}$ = .18 radian

$|(\theta_G)_{ON}|$ = .10 radian

Three variables have been investigated in this analysis. They are: the aerodynamic and gravitational unbalance torque, the balloon rotational rate and the gondola angle at which the azimuth motor goes off. The range of these variables is as follows:

$0 \leq |T_\alpha| \leq$ .20 ft. lb.

$0 \leq |\dot{\theta}_B| \leq$ .02 rad./sec.

$.08 \leq |(\theta_G)_{OFF}| \leq$ .10 radian

5.3 Results

The steady-state operating characteristics of the "Polariscope I" azimuth control cycle are presented in Figure 5.1. Angular velocities and positions of the balloon, the gondola and the inertia wheel are shown versus time during the cycle. The angular velocities vary linearly during each interval of time in the cycle, while the angular positions vary in a parabolic manner. The same initial and end conditions occur for each of the three velocities, and the gondola position. A cycle occurs between two successive points when the azimuth control motor goes on.

Figures 5.1, 5.2, and 5.3 show the operating characteristics of the azimuth control cycle for a balloon velocity of .02 radians per second and a zero aerodynamic and gravitational unbalance torque. The three figures show the effect of various azimuth motor-off conditions. Figure 5.1 shows the characteristics of a symmetrical on-off control where the gondola angle is .10 radian. Figure 5.2 shows the characteristics of a control with ten per cent hysteresis, that is a gondola angle of .09 radians at the azimuth motor "off" condition. A twenty per cent hysteresis control is shown in Figure 5.3. Single-stop azimuth

control operation occurs for the symmetrical and the ten per cent hysteresis controls while double-stop operation occurs for twenty per cent hysteresis. The azimuth motor operates only at positive gondola positions for single-stop operation while successive positive and negative gondola positions occur for double-stop operation. The smallest azimuth motor percentage operating time occurs for a control with ten per cent hysteresis. The azimuth motor operates a large percentage of the time when double-stop operation occurs. This type of operation should be avoided when minimum use of electrical power is required.

The operating characteristics of a steady-state azimuth control cycle with ten per cent hysteresis and a balloon rotational velocity of .01 radians per second are shown in Figure 5.4. Reduction in the balloon rotational rate results in a reduction in azimuth motor operating time. This is shown in Figure 5.5, which presents azimuth motor "on" time in per cent versus balloon angular velocity. An increase in the aerodynamic and gravitational unbalance torque is shown to increase the percentage motor operating time.

Figure 5.6 shows the transient-state azimuth control cycle characteristics. Initial and final conditions of the cycle are shown for various aerodynamic and gravitational unbalance torques. Stable operation is shown to exist for initial gondola angular velocities both greater than, and less than the steady-state value as the gondola velocity tends toward the steady-state value for all initial conditions. The final conditions of the cycle are always nearer the steady-state condition than the initial conditions, thus stable operation is shown to exist for all initial gondola velocities.

5.4 Conclusions

A nearly symmetrical azimuth on-off control cycle with approximately ten per cent hysteresis is desired for the "Polariscope I" balloon-telescope system. This gives a stable single-stop type of operation which results in least operating time of the azimuth control motor. An average azimuth motor operating time of approximately five per cent can be achieved with this system. The total electrical power required for the control system of a three-axis system is as low as that of any other system, thus achieving minimum battery and system weight.

REFERENCES

1. Nidey, R. A., Chapter 8 in "Proceedings of the Workshop on Scientific Ballooning", National Center for Atmospheric Research, Boulder, Colorado, 1963.

2. "A Technical Proposal for the Indiana University High Altitude Astrophysical Research Program", Report Number 7813, Part I, September, 1960, Mc Donnell Aircraft Corporation, Figure I.

3. Gehrels, Thomas, and Teska, Thomas M., "The Wavelength Dependence of Polarization", Applied Optics, Volume 2, January, 1963, Pages 67 - 77.

LIST OF NOMENCLATURE

Symbol	Definition	Units
I	Moment of Inertia	$ft.lb.sec.^2$
k	Shroud Line Torsional Spring Constant	ft.lb./rad.
n	Time Interval Number	none
t	Time	sec.
T	Torque	ft.lb.
α	Angular Acceleration Constant	$rad./sec.^2$
θ	Angular Position	radians
$\dot{\theta}$	Angular Velocity	rad./sec.
$\ddot{\theta}$	Angular Acceleration	$rad./sec.^2$

Subscript	Definition
0	Initial Condition (t=0)
1,2,3---	Time Interval Numbers
a	Aerodynamic and Gravitational Unbalance
b	Azimuth Shaft and Gear Box Friction
B	Balloon
C	Connecting Link
G	Gondola
GW	Gondola and Inertia Wheel as a Unit
i	Final Condition of Interval ($t = t_i$)

LIST OF NOMENCLATURE (Concluded)

Subscript	Definition
M	Azimuth Motor - Gear Box Output
OFF	Azimuth Motor - Off Condition
ON	Azimuth Motor - On Condition
W	Inertia Wheel
τ	End of Cycle Condition

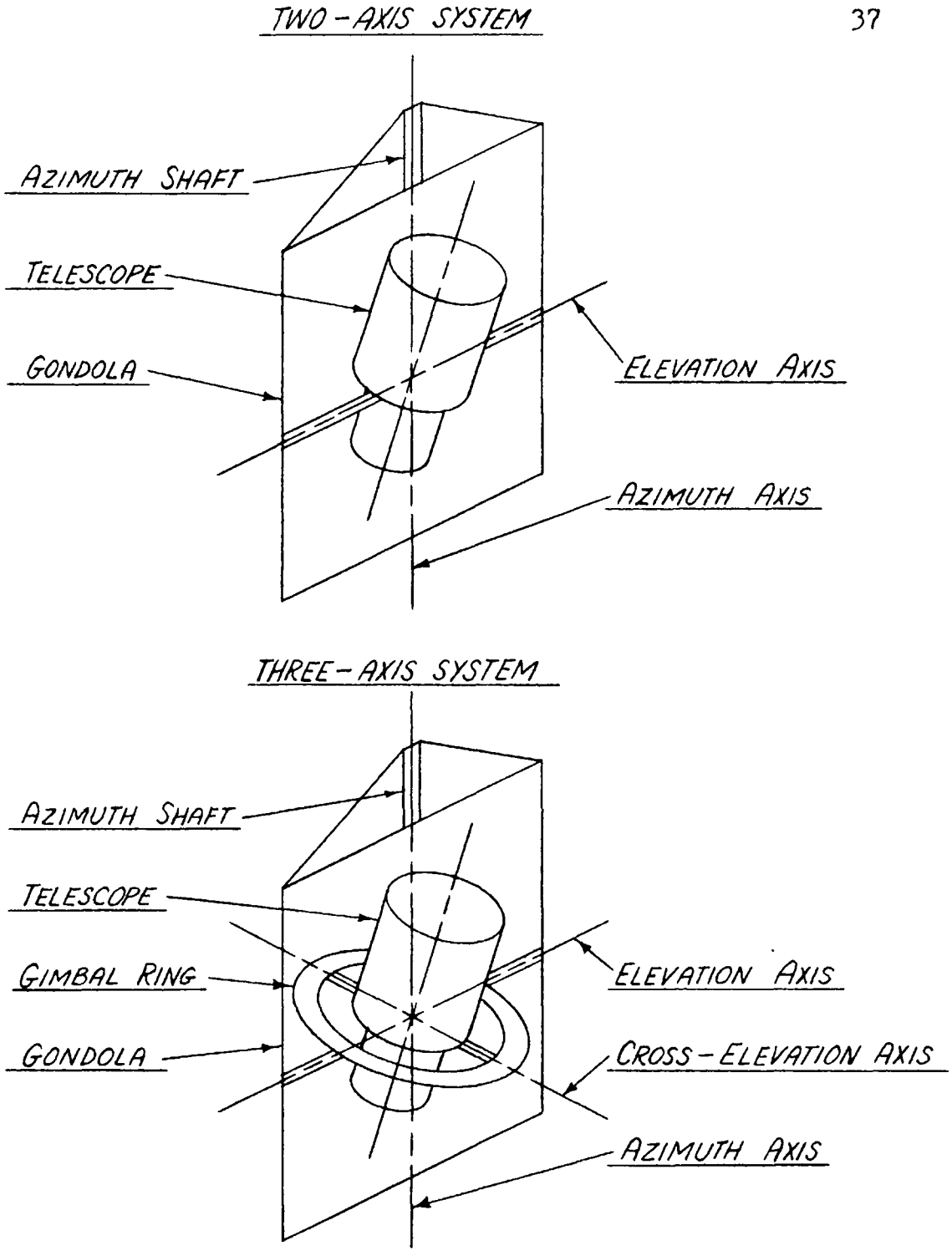

FIGURE 2.1 TELESCOPE MOUNTING CONFIGURATIONS

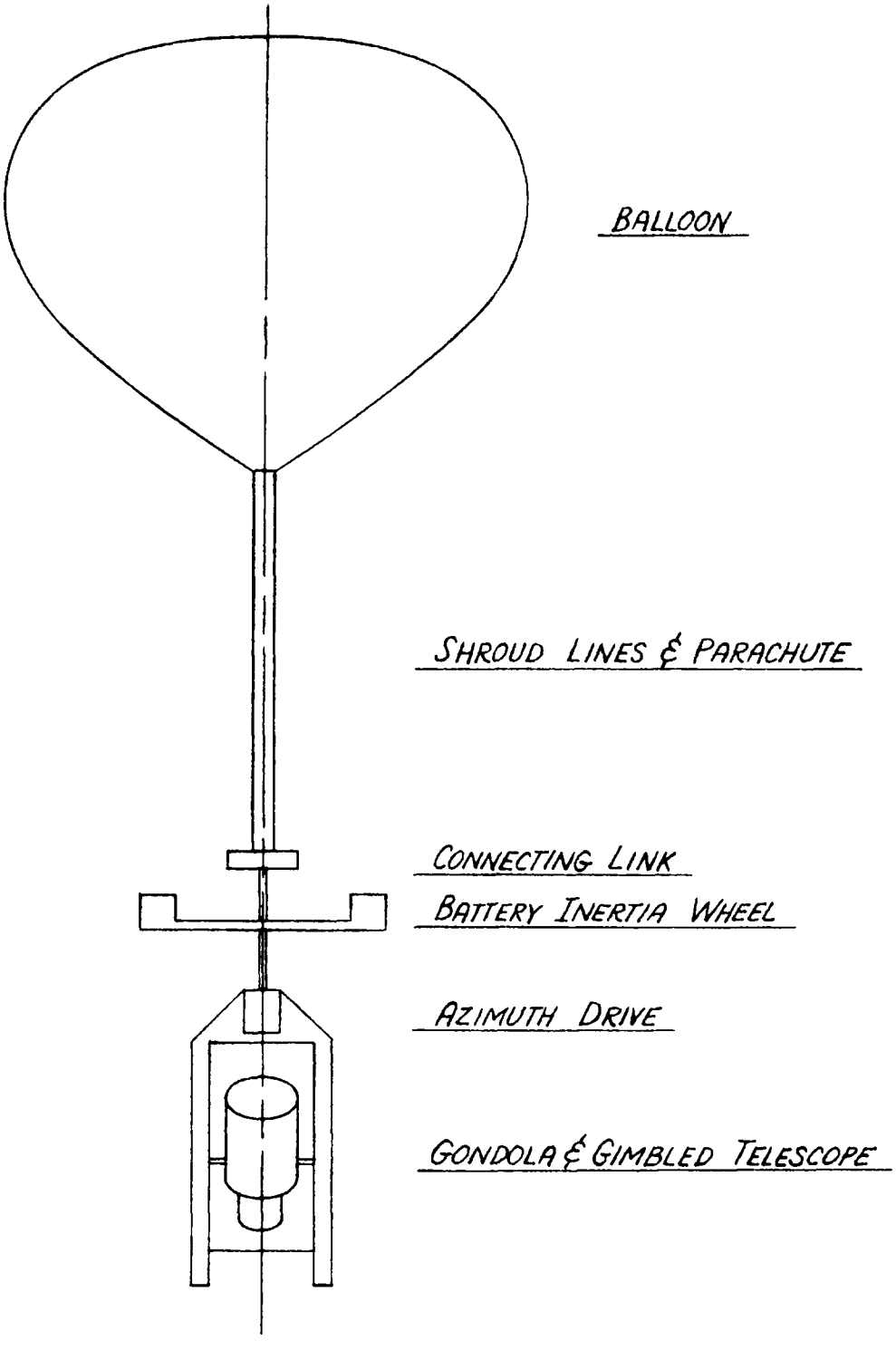

FIGURE 2.2 SCHEMATIC OF BALLOON-TELESCOPE SYSTEM

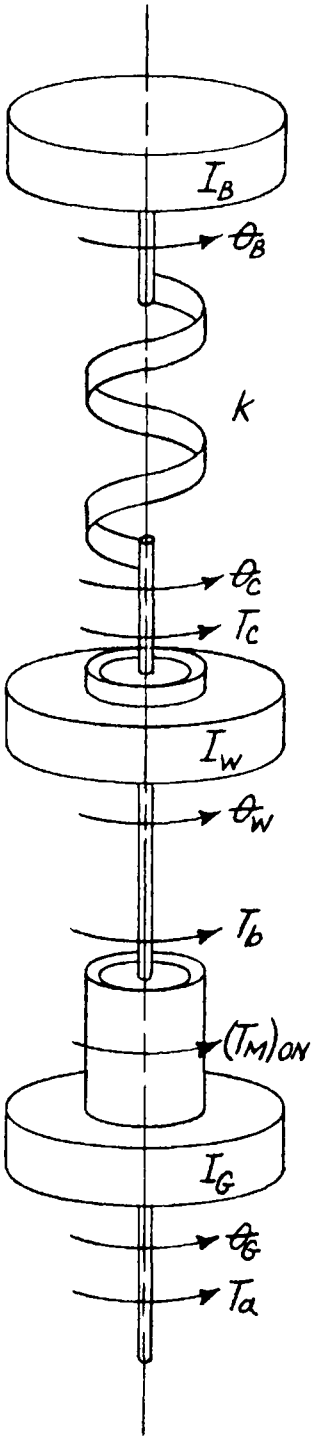

GENERAL CONDITIONS

$I_B \gg I_W$

$I_W \cong I_G$

$|T_b| > |T_c|$

$|T_c| > |T_a|$

$|(T_M)_{ON}| > |T_b|$

$K \gg |T_c|$

$\theta_c \cong \theta_B$

TYPES OF MOTION

$(\dot{\theta}_G \neq \dot{\theta}_W \neq \dot{\theta}_B)$

$(\dot{\theta}_G = \dot{\theta}_W \neq \dot{\theta}_B)$

$(\dot{\theta}_G = \dot{\theta}_W = \dot{\theta}_B)$

FIGURE 3.1 MODEL OF AZIMUTH SYSTEM

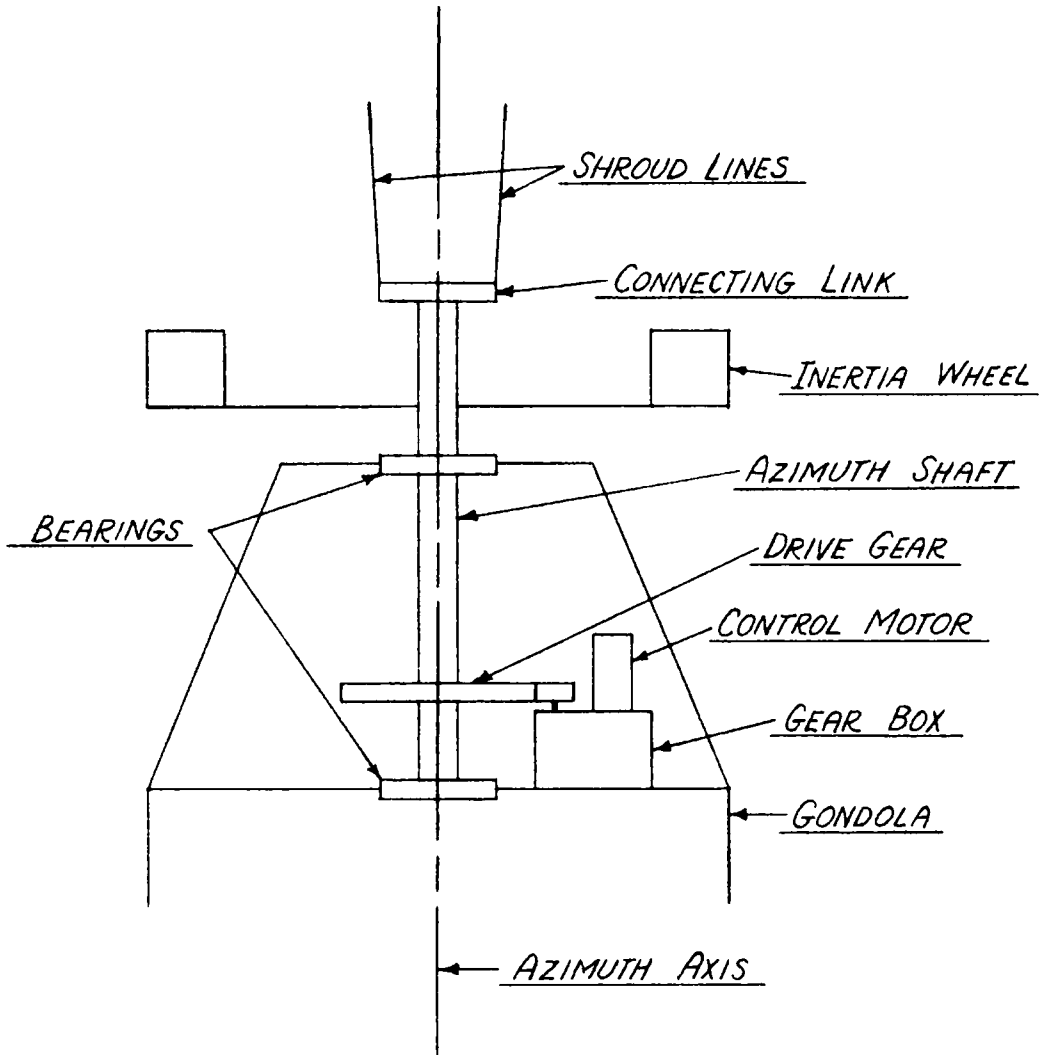

FIGURE 3.2 AZIMUTH DRIVE SYSTEM

$$T_b = \pm |T_b| \text{ WHEN } (\dot{\theta}_w - \dot{\theta}_G) \gtrless 0$$

$$|T_b| = \text{CONSTANT}$$

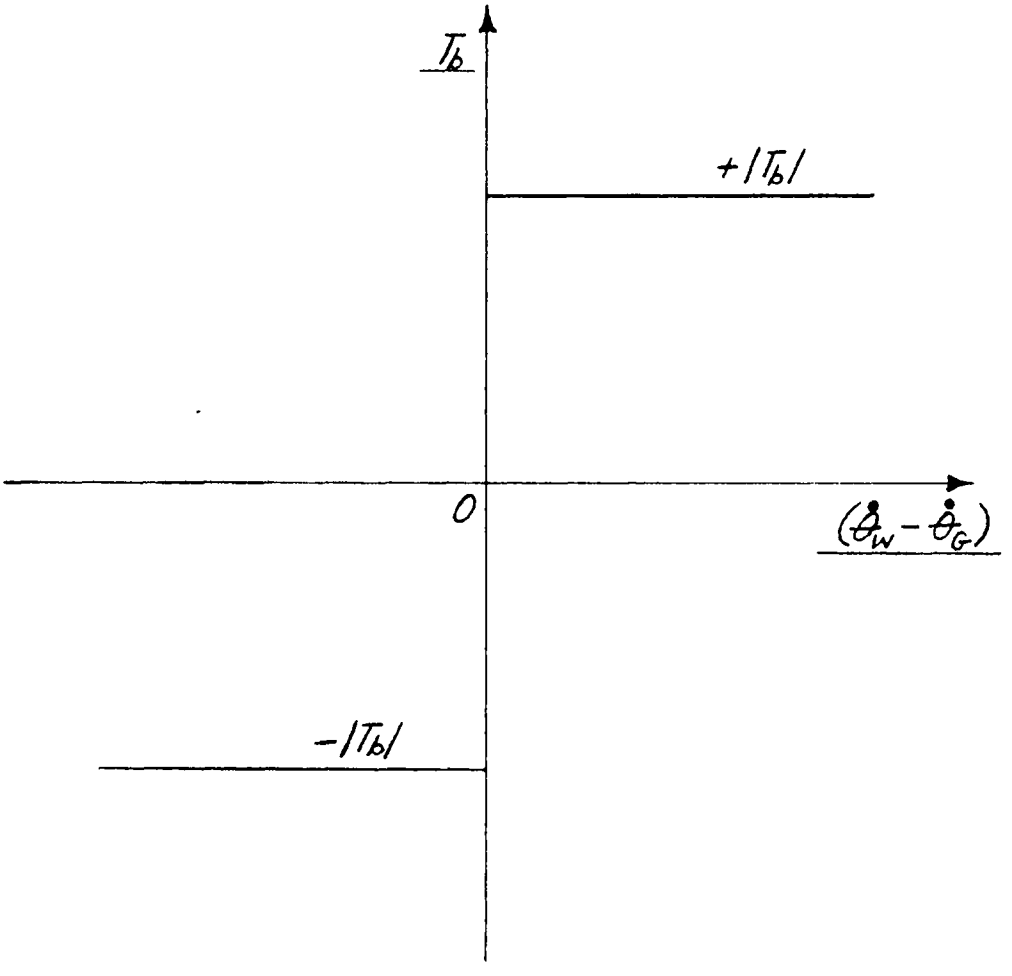

FIGURE 3.3 AZIMUTH SHAFT & GEAR BOX FRICTIONAL TORQUE

$$T_C = \pm |T_C| \text{ WHEN } (\dot{\theta}_B - \dot{\theta}_W) \gtrless 0$$

$$|T_C| = \text{CONSTANT}$$

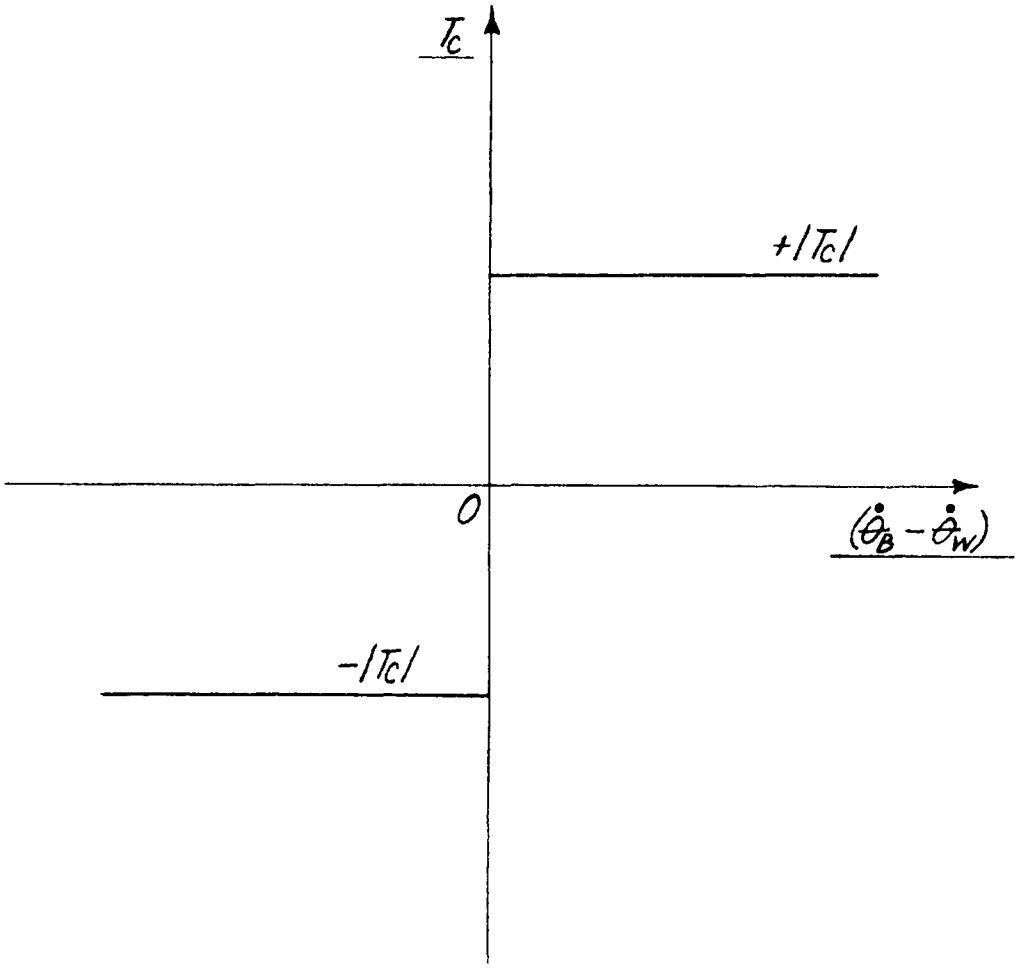

FIGURE 3.4 CONNECTING LINK FRICTIONAL TORQUE

$$|(T_M)_{ON}| = \text{CONSTANT}$$
$$(T_M)_{OFF} = 0$$

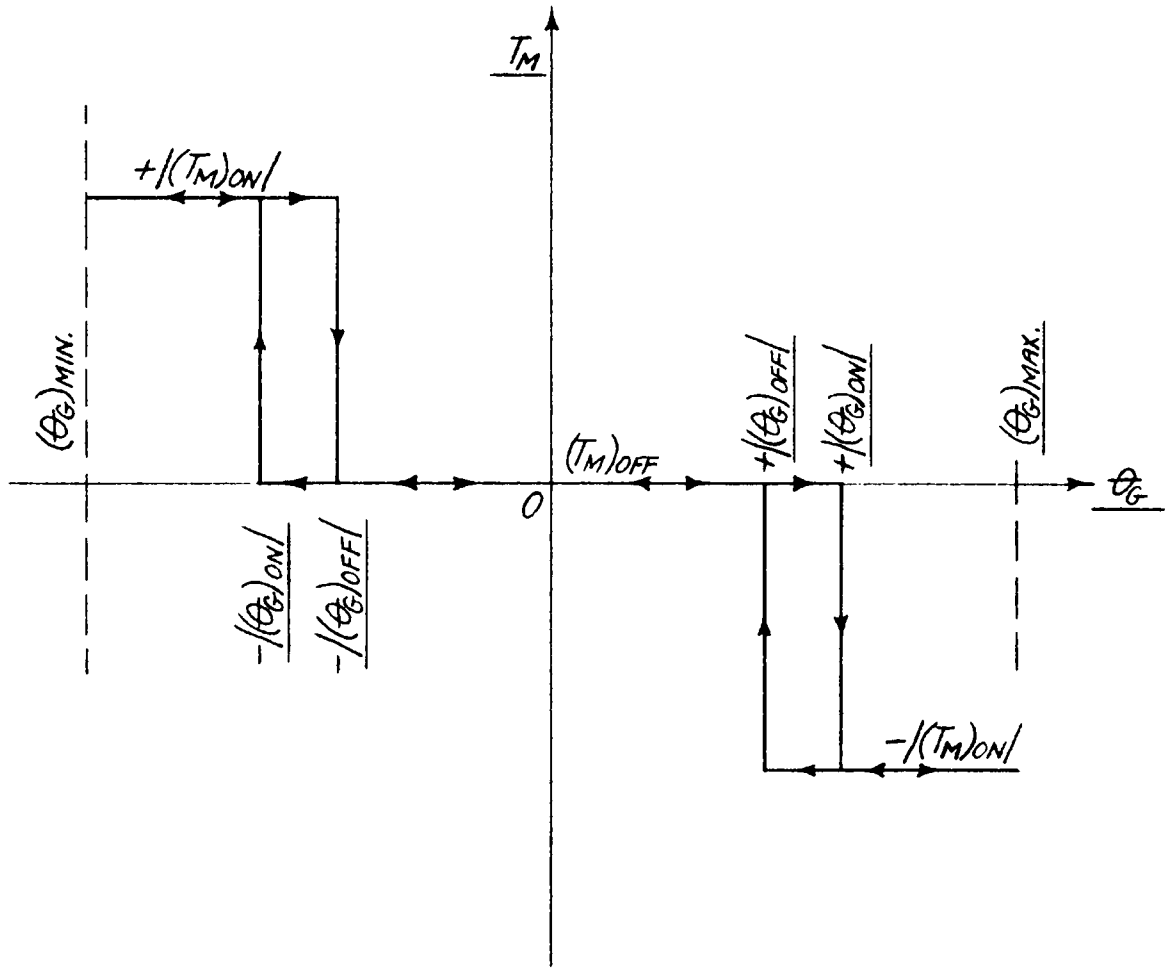

FIGURE 3.5 AZIMUTH MOTOR-GEAR BOX OUTPUT TORQUE

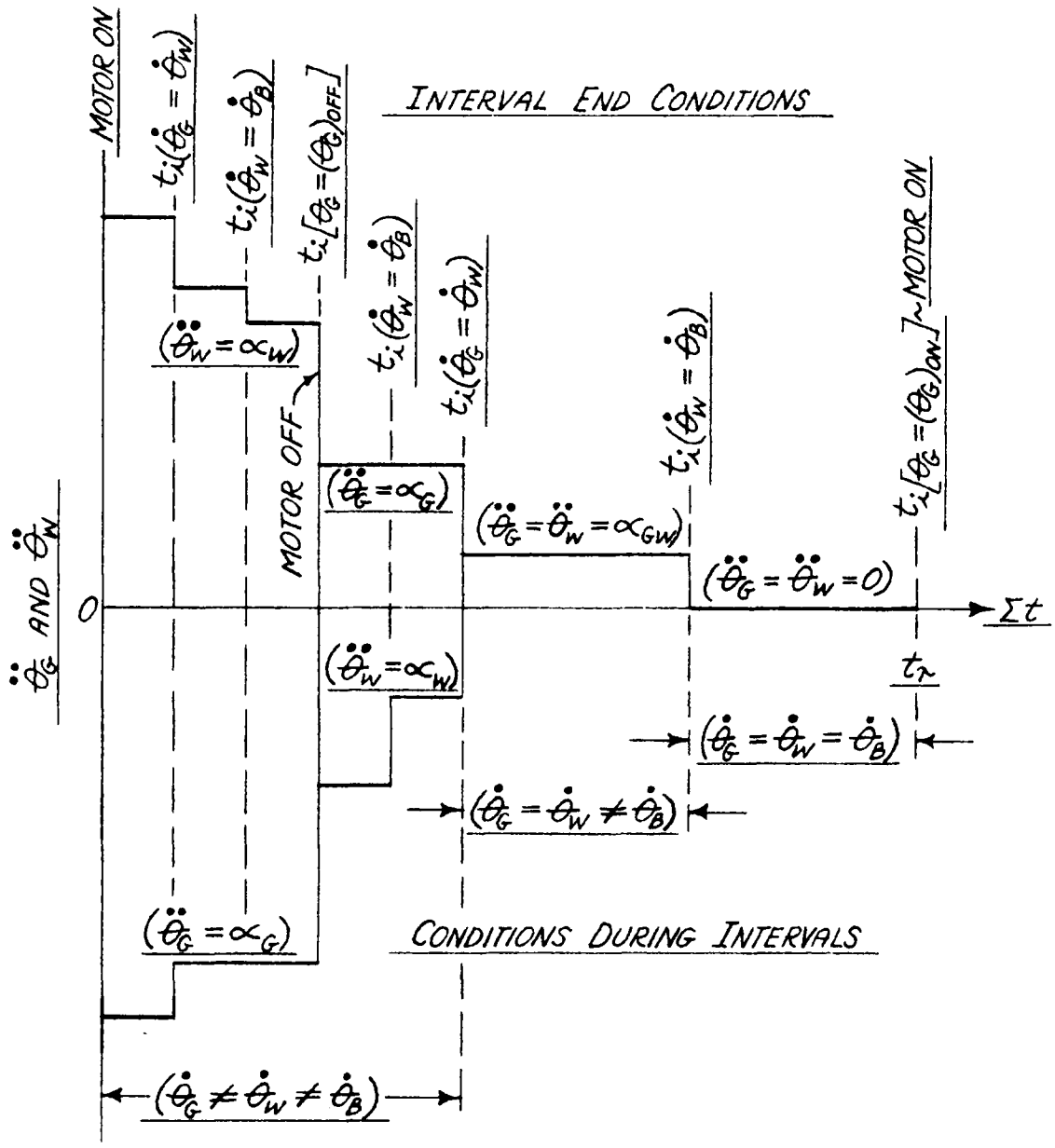

FIGURE 4.1 TYPICAL AZIMUTH CONTROL CYCLE

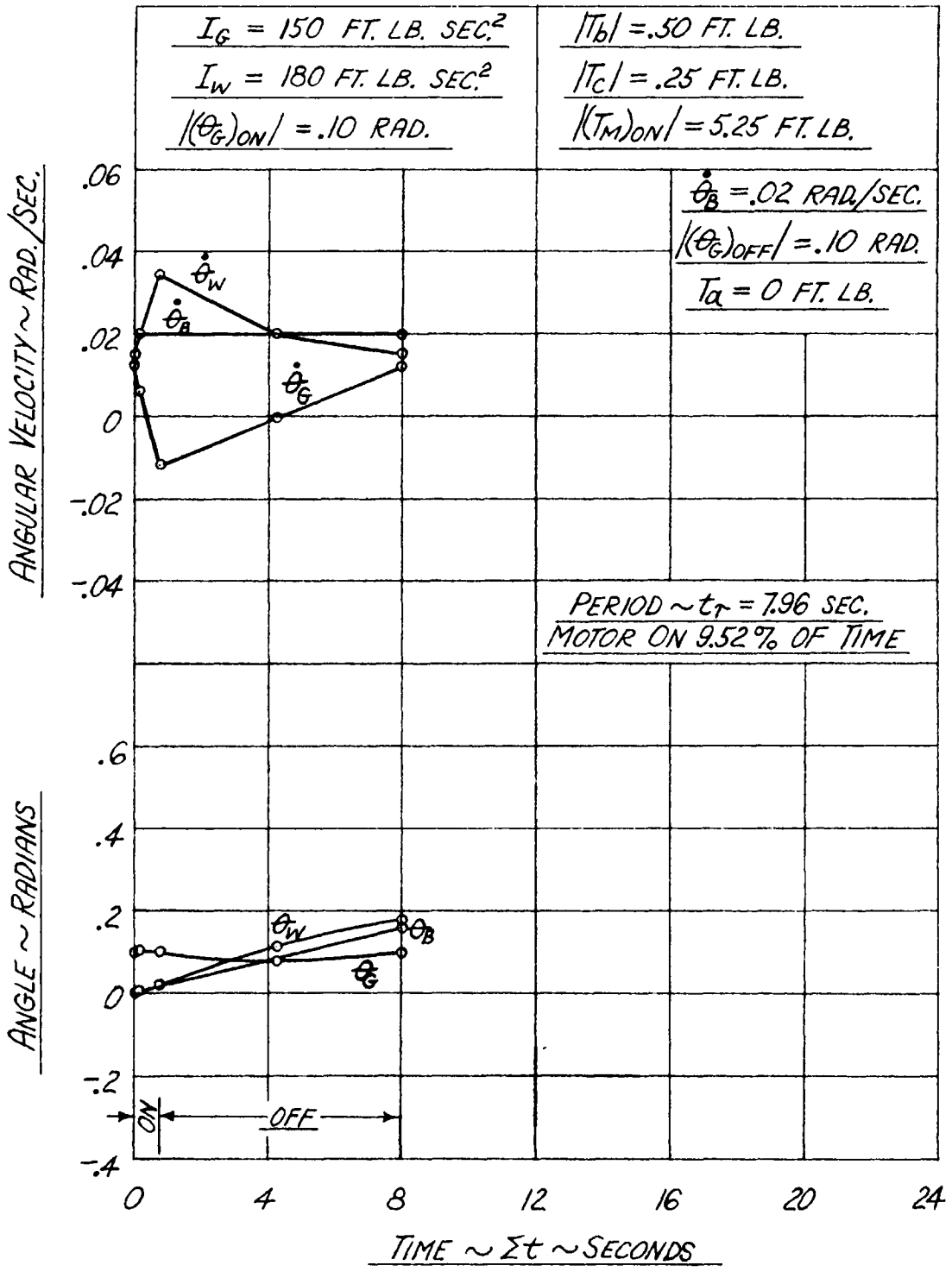

FIGURE 5.1 STEADY-STATE AZIMUTH CONTROL CYCLE

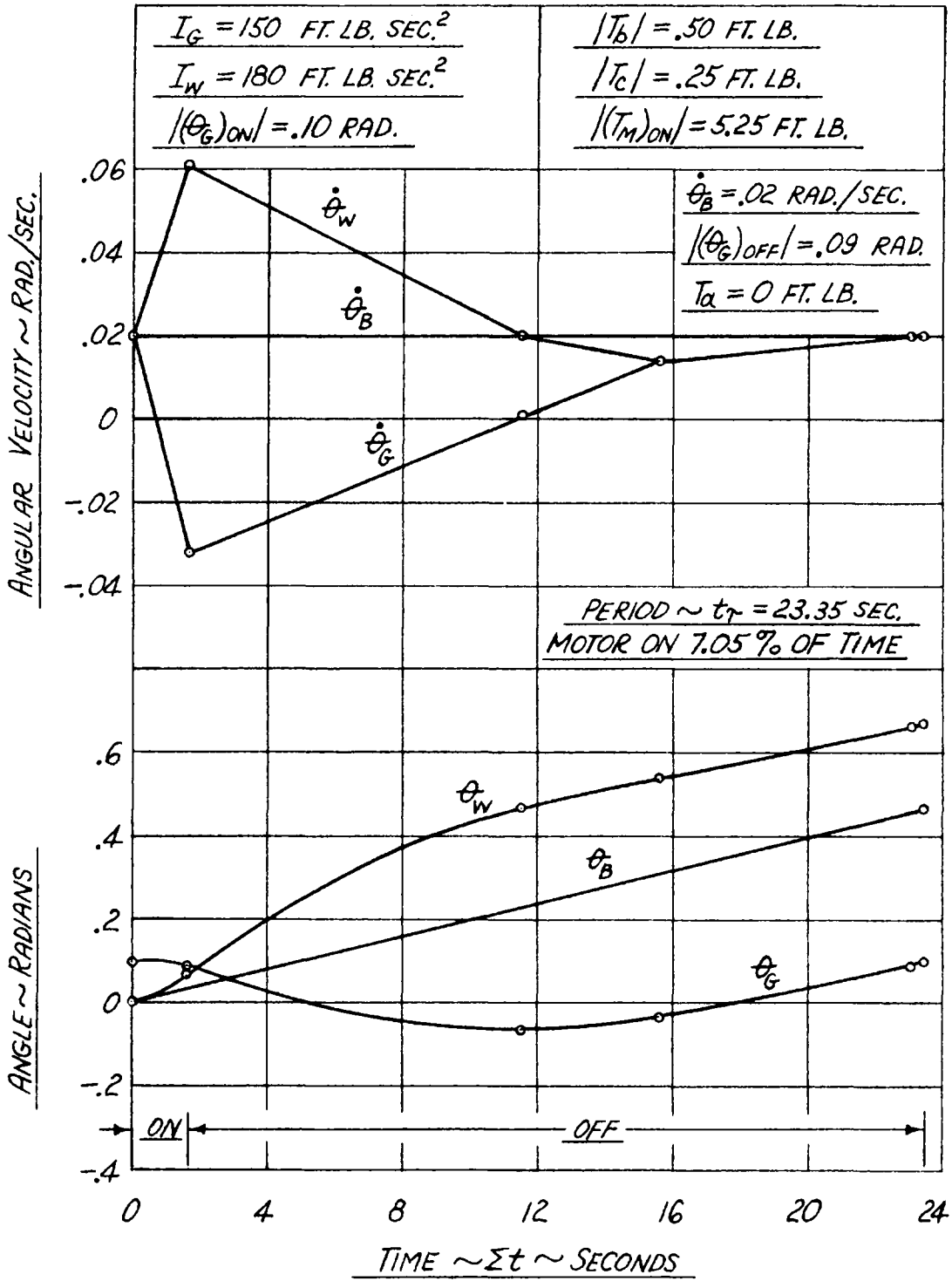

FIGURE 5.2 STEADY-STATE AZIMUTH CONTROL CYCLE

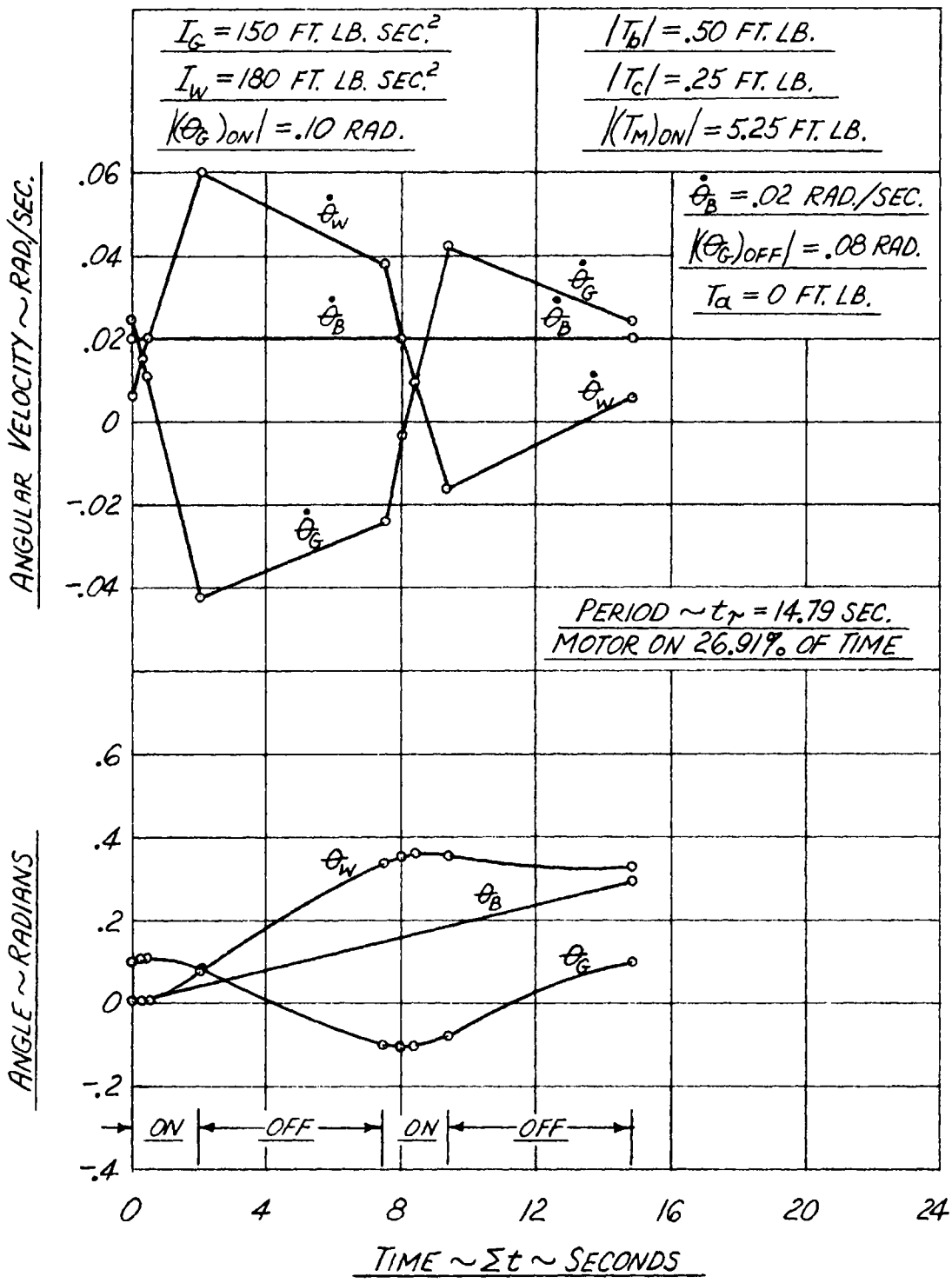

FIGURE 5.3 STEADY-STATE AZIMUTH CONTROL CYCLE

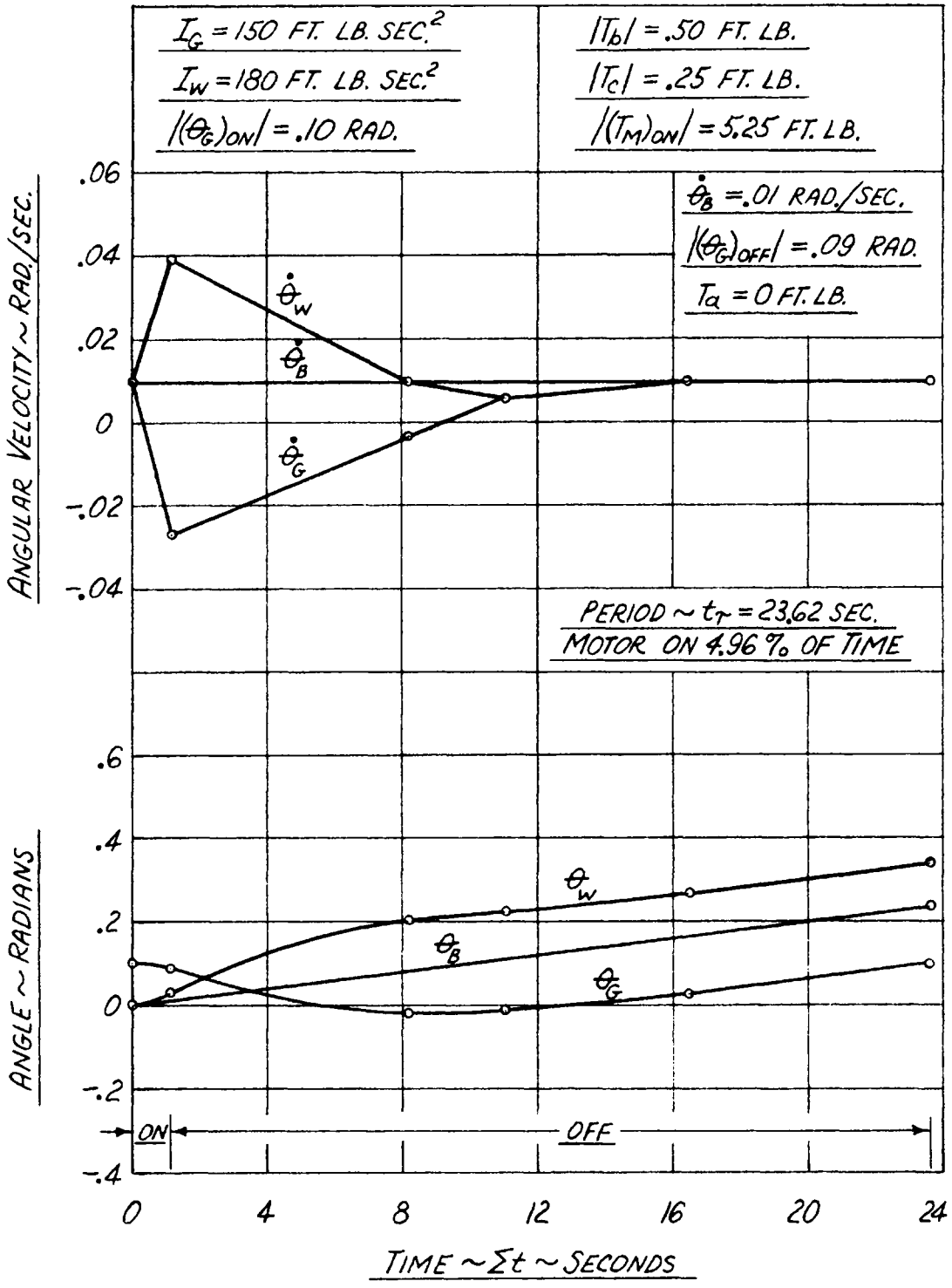

FIGURE 5.4 STEADY-STATE AZIMUTH CONTROL CYCLE

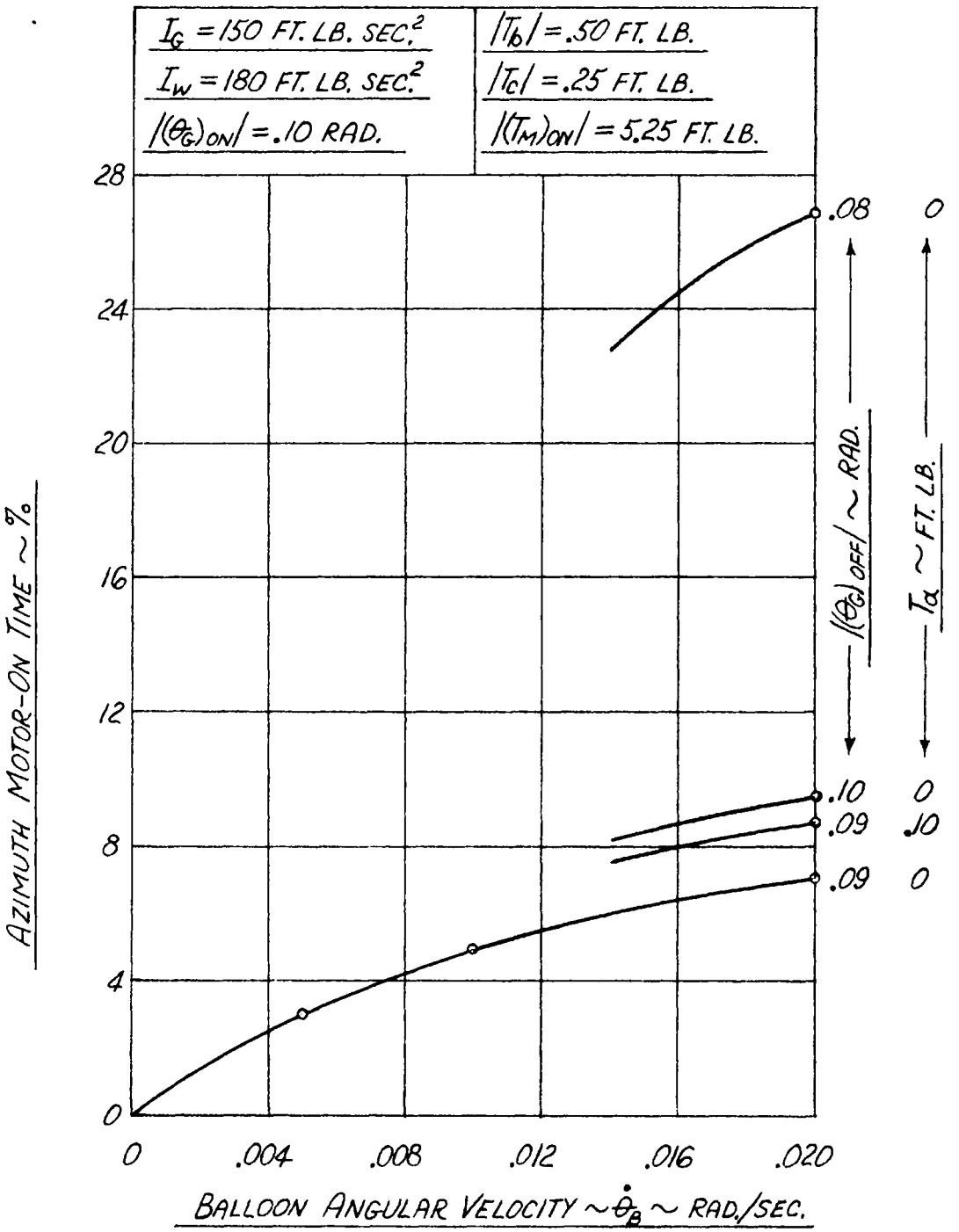

FIGURE 5.5 STEADY-STATE AZIMUTH CONTROL PERFORMANCE

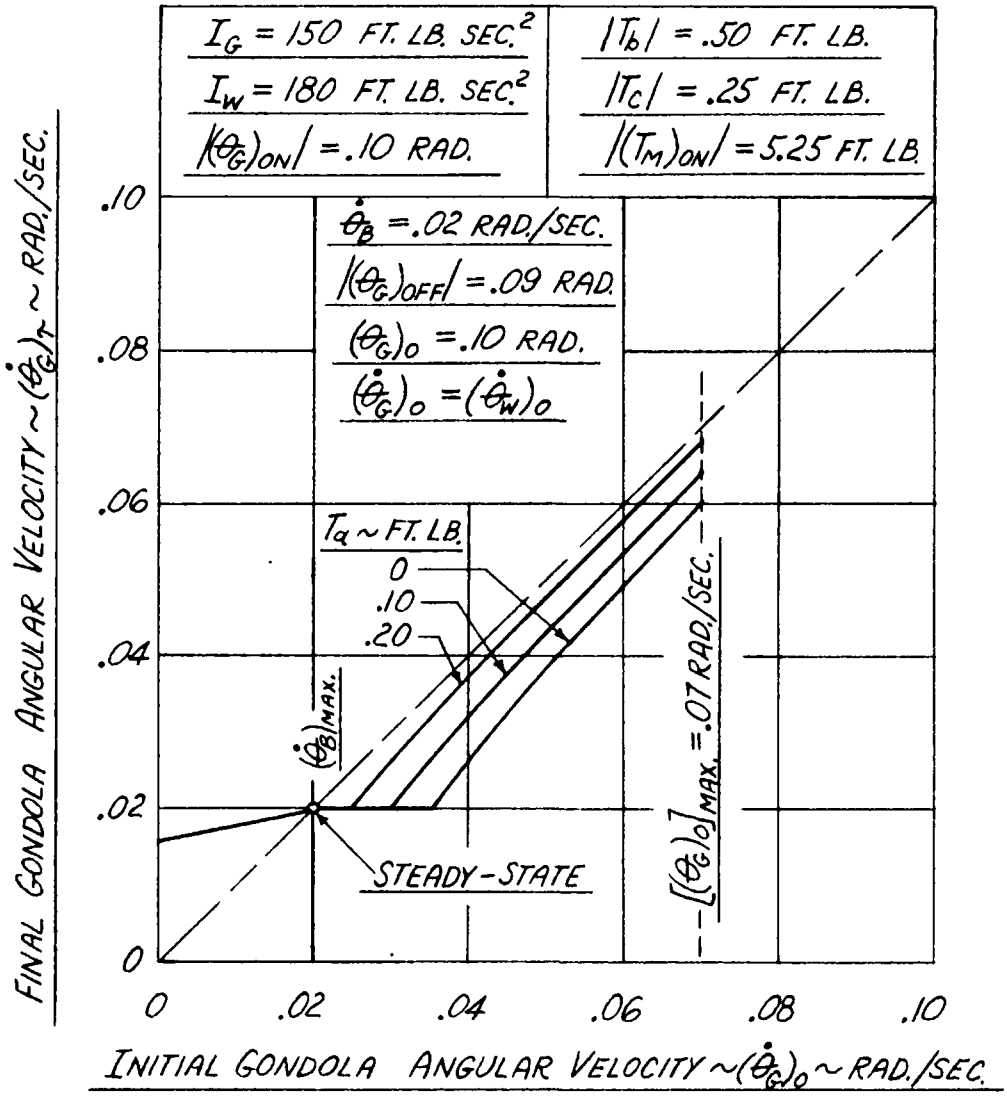

FIGURE 5.6 TRANSIENT-STATE AZIMUTH CONTROL CYCLE

TABLE 4.1 CALCULATION PROCEDURE

a. GENERAL DATA FOR $[(\theta_B)_{01}]=0$

1	2	3	4	5	6	7	8	9
n	t_0	I_G	I_W	$(\theta_G)_0$	$(\theta_W)_0$	$(\dot\theta_G)_0$	$(\dot\theta_W)_0$	$\dot\theta_B$
	SEC.	FT. LB. SEC.^{2} →		RAD. →	→	RAD./SEC. →	→	→
TIME INTERVAL	$(t_0)_1=0$			I. COND. →	→	→	→	
	(43)′ OR (69)′			(55)′ OR (78)′	(59)′ OR (79)′	(48)′ OR (74)′	(50)′ OR (74)′	

	10	11	12	13	14	15	16	17
n	$(\dot\theta_W-\dot\theta_G)_0$	$(\dot\theta_B-\dot\theta_W)_0$	$\lvert T_a\rvert$	$\lvert T_b\rvert$	$\lvert T_c\rvert$	$\lvert T_M\rvert_{ON}$	$\lvert\theta_G\rvert_{OFF}$	$\lvert\theta_G\rvert_{ON}$
	RAD./SEC. →	→	FT. LB. →	→	→	→	RAD. →	→
①	⑧−⑦	⑨−⑧						

TABLE 4.1 (CONTINUED)

b. SOLUTION OF EQUATIONS 4.2, 4.3, 4.14 AND 4.15 DURING TIME INTERVAL, $(\dot{\theta}_G \neq \dot{\theta}_W \neq \dot{\theta}_B)$

n	18 T_a FT. LB.	19 T_b	20 T_c	21 T_M	22 $(T_b + T_M)$
		(SEE FIGURE 3.3)	(SEE FIGURE 3.4)	(SEE FIGURE 3.5)	
①	±⑫	$T_b = \pm$⑬ FOR ⑩ ≷ 0	$T_c = \pm$⑭ FOR ⑪ ≷ 0	$T_M = \pm$⑮ OR $T_M = 0$	⑲ + ㉑

n	23 $(T_a + T_b + T_m)$ FT. LB.	24 $\left(\frac{T_b + T_M}{I_W}\right)$ RAD./SEC.^{2}	25 α_G	26 $\left(\frac{T_c}{I_W}\right)$	27 α_W	28 $(\alpha_G - \alpha_W)$	29 $t_i(\dot{\theta}_G = \dot{\theta}_W)$ SEC.	30 $t_i(\dot{\theta}_W = \dot{\theta}_B)$
①	⑱ + ㉒	㉒/④	㉓/③	⑳/④	㉖ − ㉔	㉕ − ㉗	⑩/㉘	⑪/㉗

TABLE 4.1 (CONTINUED)

C. SOLUTION OF EQUATIONS 4.16 AND 4.17 DURING TIME INTERVAL, $(\dot{\theta}_G \neq \dot{\theta}_W \neq \dot{\theta}_B)$

n	31 $\frac{(\dot{\theta}_G)_0}{\alpha_G}$ SEC.	32 SEC.^{2}	33 $[(\theta_G)_0 - (\theta_G)_{OFF}]$ RAD. (FOR $\lvert T_M \rvert > 0$)	34 SEC.^{2} →	35 →	36 SEC. →	37 $t_{i[\theta_G=(\theta_G)_{OFF}]}$ → (LOWEST, >0)
(1)	(7)/(25)	(31)^2	(5) ∓ (16)	2(33)/(25)	(32) − (34)	√(35)	± (36) − (31)

n	38 $[(\theta_G)_0 - (\theta_G)_{ON}]$ RAD. (FOR $T_M = 0$)	39 SEC.^{2} →	40 →	41 SEC. →	42 $t_{i[\theta_G=(\theta_G)_{ON}]}$ (LOWEST, >0) →	43 t_i →
(1)	(5) ∓ (17)	2(38)/(25)	(32) − (39)	√(40)	± (41) − (31)	(29), (30), (31) OR (42)

TABLE 4.1 (CONTINUED)

d. SOLUTION OF EQUATIONS 4.4, 4.5, 4.6, 4.7, 4.20 AND 4.22 DURING TIME INTERVAL, $(\dot{\theta}_G \neq \dot{\theta}_W \neq \dot{\theta}_B)$

n	44 t SEC. →	45 Σt	46 t^2 SEC.^{2}	47 $(\alpha_G)\,t$ RAD./SEC. →	48 $\dot{\theta}_G$	49 $(\alpha_W)\,t$	50 $\dot{\theta}_W$ →	51 $\dot{\theta}_B$ RAD. $[(\theta_B)_0]_1=0$
①	$0 \le t \le$ (43)	(2)+(44) OR (45)′+(44)	(44)^2	(25)(44)	(7)+(47) OR (48)′+(47)	(27)(44)	(8)+(49) OR (50)′+(49)	(9)(45)

n	52 $(\dot{\theta}_G)_0\,t$ RAD. →	53 $(\alpha_G)\frac{t^2}{2}$	54	55 θ_G	56 $(\dot{\theta}_W)_0\,t$	57 $(\alpha_W)\frac{t^2}{2}$	58	59 θ_W →
①	(7)(44)	$\frac{(25)(46)}{2}$	(52)+(53)	(5)+(54) OR (55)′+(54)	(8)(44)	$\frac{(27)(46)}{2}$	(56)+(57)	(6)+(58) OR (59)′+(58)

TABLE 4.1 (CONTINUED)

e. SOLUTION OF EQUATIONS 4.8 AND 4.18 DURING TIME INTERVAL, $(\dot{\theta}_G = \dot{\theta}_W \neq \dot{\theta}_B)$

n	60 $(I_G + I_W)$ FT. LB. SEC.^{2}	61 $(T_\alpha + T_c)$ FT. LB.	62 α_{GW} RAD./SEC.^{2}	63 $[(\theta_G)_0 - (\theta_G)_{ON}]$ RAD.	64 SEC.^{2}
①	③ + ④	⑱ + ⑳	⑥₁/⑥₀	⑤ ∓ ⑰	2 ⑥₃/⑥₂

n	65 $\frac{(\dot{\theta}_G)_0}{\alpha_{GW}}$ SEC.	66 SEC.^{2}	67 →	68 SEC.	69 $t_i[\theta_G = (\theta_G)_{ON}]$ →
①	⑦/⑥₂	⑥₅^2	⑥₆ − ⑥₄	$\sqrt{⑥₇}$	(LOWEST, >0) ± ⑥₈ − ⑥₅

TABLE 4.1 (CONTINUED)

f. SOLUTION OF EQUATIONS 4.9, 4.10, 4.11, 4.20 AND 4.22 DURING TIME INTERVAL, $(\dot{\theta}_G = \dot{\theta}_W \neq \dot{\theta}_B)$

n	70 t SEC. →	71 Σt	72 t^2 SEC.^{2}	73 $(\alpha_{GW})t$ RAD./SEC.	74 $\dot{\theta}_G = \dot{\theta}_W$ →	75 $(\dot{\theta}_G)_0 t$ RAD.
①	$0 \leq t \leq$ (69)	(2) + (70)	(70)^2	(62)(70)	(7) + (73)	(7)(70)

n	76 $(\alpha_{GW})\frac{t^2}{2}$ RAD. →	77	78 θ_G	79 θ_W	80 θ_B →
①	$\frac{(62)(72)}{2}$	(75) + (76)	(5) + (77)	(6) + (77)	$[(\theta_B)_0]_1 = 0$ (9)(71)

TABLE 4.1 (CONCLUDED)

g. SOLUTION OF EQUATIONS 4.12, 4.13, 4.19, 4.20, 4.21 & 4.22 DURING TIME INTERVAL, ($\dot{\theta}_G = \dot{\theta}_W = \dot{\theta}_B$ = CONSTANT)

n	81 $[(\theta_G)_{ON} - (\theta_G)_0]$ RAD.	82 $t_i[\theta_G = (\theta_G)_{ON}]$ SEC.	83 t	84 Σt	85 $(\dot{\theta}_B)t$ RAD.
①	±⑰ − ⑤	⑧① / ⑨	$0 \le t \le$ ⑧②	② + ⑧③	⑨ ⑧③

n	86 θ_G RAD.	87 θ_W	88 θ_B	89 $\dot{\theta}_G = \dot{\theta}_W = \dot{\theta}_B$ RAD./SEC.	90 t_f SEC.
①	⑤ + ⑧⑤	⑥ + ⑧⑤	$[(\theta_B)_0]_1 = 0$ ⑨ ⑧④	⑨	② + ④③, ② + ⑥⑨ OR ② + ⑧②